



Continuous and discontinuous grain-boundary wetting in $\text{Zn}_x\text{Al}_{1-x}$

Boris B. Straumal,^{1,2} Alena S. Gornakova,¹ Olga A. Kogtenkova,¹ Svetlana G. Protasova,¹ Vera G. Sursaeva,¹ and Brigitte Baretzky²

¹*Institute of Solid State Physics, Russian Academy of Sciences, Chernogolovka, Moscow District 142432, Russia*

²*Max-Planck-Institut für Metallforschung, Heisenbergstrasse 3, D-70569 Stuttgart, Germany*

(Received 6 November 2007; published 12 August 2008)

Temperature dependences of the contact angle $\theta(T)$ between (i) specially grown tilt grain boundaries (GBs) in Al and the Zn-rich melt; (ii) tilt GBs in Zn and the Al-rich melt; and (iii) tilt GBs in Zn and the Al-based solid solution (Al)^{''} were measured using scanning electron microscopy and light microscopy. θ decreases with increasing T in all cases and reaches zero (complete wetting) at a certain temperature T_w in cases (i) and (ii). The wetting transformation for Al GBs is discontinuous (first order): $\theta(T)$ dependence is convex, $d\theta/dT$ has a break at T_w , and $\theta \sim [(T - T_w)/T_w]^{1/2}$. The wetting transformation for Zn GBs is continuous: $\theta(T)$ dependence is concave, $d\theta/dT$ is continuous at T_w , and $\theta \sim [(T - T_w)/T_w]^{3/2}$. For the Zn GBs in contact with a second solid phase (Al)^{''}, $\theta(T)$ dependence is concave and $\theta \sim [(T - T_w)/T_w]^{3/2}$ for the extrapolated T_w . The observed change from the discontinuous wetting transition for GBs in a metal with a higher melting point (Al) to the continuous one for GBs in a metal with a lower melting point (Zn) is explained using the approach proposed in [Pandit *et al.*, Phys. Rev. B **26**, 5112 (1982)]. The validity of this approach and critical exponent of 3/2 may indicate that GB wetting in the Zn-rich alloys is governed by the long-range forces.

DOI: [10.1103/PhysRevB.78.054202](https://doi.org/10.1103/PhysRevB.78.054202)

PACS number(s): 68.08.Bc, 68.35.Md, 68.35.Rh

I. INTRODUCTION

For the liquid droplet on a solid substrate, two situations are possible. If a liquid spreads on the surface, then one can speak about full (or complete) wetting. The contact angle between liquid and solid in this case is zero. If a liquid droplet does not spread and forms a finite contact angle, then it is a partial (or incomplete) wetting. Cahn¹ and Ebner and Saam² first assumed that the (reversible) transition from incomplete to complete wetting can proceed with increasing temperature and it is a true surface phase transformation. Cahn proposed that in the three-phase area of the phase diagram close to the critical point T_c , where two phases become undistinguishable, the wetting transition should occur. This is due to the fact that if α' and α'' phases become undistinguishable at T_c and the β phase remains unchanged, then the energy of the α'/α'' interphase boundary $\sigma_{\alpha'\alpha''}$ tends to zero at the temperature $T \rightarrow T_c$. The energy $\sigma_{\alpha'\alpha''}$ would always reduce to lower than the energy of the α'/β (or α''/β) boundary $\sigma_{\alpha\beta}$ above a specified temperature T_w , which is close enough to T_c . The reviews of the works on the wetting phase transitions can be found in Refs. 3–7.

The transition from incomplete to the complete wetting can also be observed within the intercrystalline boundaries [or grain boundaries (GBs)] if the energy of two solid-liquid interfaces $2\sigma_{\text{SL}}$ reduces to lower than the GB energy $\sigma_{\text{GB}} > 2\sigma_{\text{SL}}$. Cahn's idea¹ was the “driving force” for the experimental finding of GB wetting phase transformations, initially made in Zn-Sn, Zn-Sn-Pb, and Ag-Pb polycrystals.^{8,9} At a later state, the original experimental data were reconsidered from this point of view and numerous indications on the GB wetting phase transformations were found, particularly for Zn-Sn, Al-Cd, Al-In, Al-Pb,¹⁰ W-Ni, W-Cu, W-Fe, Mo-Ni, Mo-Cu, and Mo-Fe (Ref. 11) polycrystals. The exact measurements of the temperature dependence for the GB contact angle with the melt were made using the individual GBs in

the specially grown bicrystals in the Cu-In,¹² Al-Sn,¹³ and Zn-Sn (Ref. 14) systems. Cahn's generic phase diagram¹ also predicted that the tie line of the wetting transition in the two-phase region continues in the one-phase (solid solution) area as a prewetting line. Between the prewetting line and the solubility limit for a solid solution, the surface contains a thin (liquidlike) layer of a phase, which is not stable in the bulk. The experimental evidence of such prewetting (or pre-melting) layers was also found in GBs in the Fe-Si-Zn,^{15–17} Cu-Bi,¹⁸ and Al-Zn (Ref. 19) systems and semiconductors such as Y_2O_3 -doped AlN,²⁰ La-doped SrTiO_3 ,²¹ Bi_2O_3 -doped ZnO ,^{22,23} and Ca-doped Si_3N_4 .²⁴ Wetting and prewetting (premelting) phase transformations drastically change the GB properties such as diffusivity,^{15–18} mobility,²⁵ strength,¹⁸ segregation,¹⁸ and conductivity.^{20–24,26} GB wetting phenomena play an important role for the liquid-phase sintering of metals and ceramics,^{27,28} semisolid metal processing,²⁹ thixotropic casting,³⁰ and the exploitation of heat-exchanger tubes filled with liquid metal in nuclear plants,³¹ etc.

All these mentioned surface and GB wetting phase transformations are of first order (discontinuous), which means that discontinuity of the first derivative of surface (or GB) energy occurs at T_w . However, the wetting transitions of a higher order are also possible. In other words, the first derivative of surface (or GB) energy remains continuous at T_w , but their higher derivatives have a break. The continuous wetting phase transitions were theoretically predicted in Refs. 32–34 and for a long time remained a topic for the very intensive theoretic investigations^{35–37} (see also Ref. 7 for the review). Indeed, the continuous wetting phase transition was first observed experimentally only in 1996.^{38,39} Up to now, all continuous wetting phase transitions were observed for the alkanes in contact with methanol, water, or brine liquid/liquid systems, which are technologically important for oil recovery.^{40–45} The continuous thickness divergence of the al-

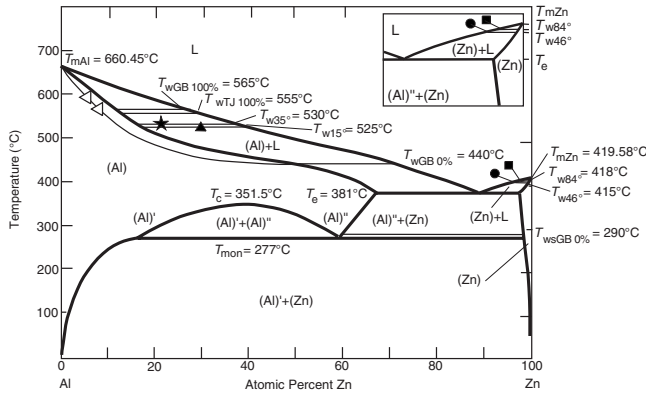


FIG. 1. Al-Zn phase diagram constructed using the data (Refs. 19 and 53–58). Thick lines denote bulk phase transformations (Ref. 57). Thin lines denote GB phase transformations (Refs. 19, 53–56, and 58). Open triangles denote TEM and DSC data for the GB prewetting line (Refs. 54 and 55). Filled star, triangle, rings, and squares denote the GB wetting temperatures obtained in this work (Figs. 4 and 5). The inset shows the Zn-rich corner of the diagram.

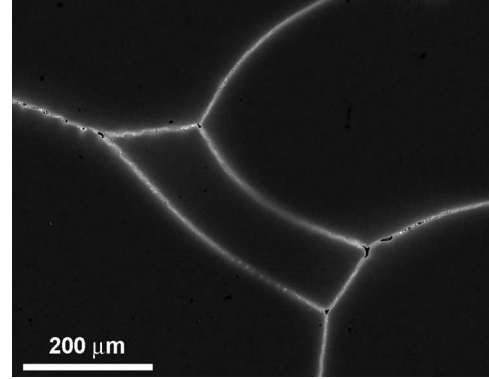


FIG. 2. SEM micrograph of the Al-5 at. % Zn alloy annealed at $T=620\text{ }^\circ\text{C}$ (i.e., above $T_{wGB100\%}=565\text{ }^\circ\text{C}$). (Al) matrix appears black; the quenched Zn-containing melt appears white.

cane layer on water or brine substrate was observed as long-range critical wetting due to the long-range van der Waals forces. It is usually preceded by the first-order thin-thick transition in the adsorbed alcane layer leading to the appearance of the mesoscopic film on the water or brine surface. These experiments supported further theoretical developments.^{46–52} However, the data^{38–45} obtained on a rather restricted number of a very similar binary liquid systems remained up to now a single array of experimental observations of continuous wetting transformations. At the end of an excellent review by Bonn and Ross,⁷ it was stated that “similar results in a different kind of system, in particular a solid substrate system, would be very interesting to see.”

This work is devoted to the experimental observation of the first-order and continuous GB wetting in the Al-Zn system using the individual GBs in the specially grown Al and Zn bicrystals. From the bulk Al-Zn phase diagram (Fig. 1), it is obvious that the Al-Zn system belongs to the “classical” Cahn’s systems with a critical point for a binary solution. It was previously observed in experiments with polycrystals that in the (Al)+L two-phase region, the GB transformation for the Al GBs wetting by Zn-containing melt occurs.¹⁹ (Al) is the Al-based Al+Zn solid solution. Below $T_{wGB0\%}=440\text{ }^\circ\text{C}$, completely wetted GBs in the Al-Zn polycrystals do not exist. $T_{wGB0\%}$ is the wetting temperature for a GB with maximal energy $\sigma_{GB\text{ max}}$. Above $T_{wGB100\%}=565\text{ }^\circ\text{C}$, all high-angle GBs in (Al) are wetted by the melt (Fig. 2).^{19,53} $T_{wGB100\%}$ is the wetting temperature for a GB with minimal energy $\sigma_{GB\text{ min}}$. Between $T_{wGB0\%}$ and $T_{wGB100\%}$, the wetting tie lines for GBs with intermediate $\sigma_{GB\text{ max}} > \sigma_{GB} > \sigma_{GB\text{ min}}$ are positioned in the (Al)+L area. GB triple junctions (TJs) become completely wetted at the temperature $T_{wTJ100\%}=555\text{ }^\circ\text{C}$ below $T_{wGB100\%}$.⁵³ According to Cahn’s generic phase diagram, the GB wetting tie lines continue as prewetting (or premelting) lines in the one-phase (Al) area. Just one prewetting line for $T_{wGB0\%}$ is shown for simplicity in Fig. 1. The experimental evidence for the existence of a GB liquid-like phase between GB prewetting line and bulk solidus line

was obtained by transmission electron microscopy (TEM) (Ref. 54) and differential scanning calorimetry (DSC) (Ref. 55) (open triangles in Fig. 1). It was also observed that the second solid phase (Al)'' can completely wet the GBs in (Zn) polycrystals.⁵⁶ (Zn) is the Zn-based Zn+Al solid solution. (Al)' and (Al)'' are the isomorphous Al-based solid solutions with low- and high-Zn content, respectively, below the critical point $T_c=351.5\text{ }^\circ\text{C}$ (Fig. 1). Below $T_{wsGB0\%}=290\text{ }^\circ\text{C}$, no (Zn) GBs completely wetted by the (Al)'' solid phase exist in the (Zn)+(Al)'' polycrystals. Above $T_{wsGB0\%}$, the (Zn) GBs completely wetted by the (Al)'' solid phase appear in the (Zn)+(Al)'' polycrystals. The amount of completely wetted (Zn) GBs increases with increasing temperature and reaches about 30% at eutectic temperature $T_e=381\text{ }^\circ\text{C}$. Thus, the majority of (Zn) GBs remain incompletely wetted by the (Al)'' solid phase at T_e and the tie line $T_{wsGB100\%}$ is not present in the (Al)''+(Zn) two-phase region of the Al-Zn phase diagram (Fig. 1). However, experimental evidence was obtained which indicated that the (Al)' phase with low-Zn concentration does not completely wet the (Zn) GBs in the (Al)'+(Zn) two-phase region below the temperature $T_{\text{mon}}=277\text{ }^\circ\text{C}$ of monotectoid transformation.⁵⁶ The same is also true for the opposite side of the (Al)'+(Zn) two-phase region.⁵⁷ In other words, the (Zn) solid phase cannot completely wet the GBs in the (Al)' phase.⁵⁸

II. EXPERIMENT

Flat Al and Zn bicrystals having a thickness of 2 mm, a width of 10 mm, and a length of 50–100 mm with individual tilt GBs were grown from the Al and Zn of 99.999 at. % purity using the modified Bridgman technique.^{59,60} Two $\langle 110 \rangle$ tilt GBs with misorientation angles $\phi=15^\circ$ and 35° in Al and three $[11\bar{2}0]$ tilt GBs with misorientation angles $\phi=11.5^\circ$, 46° , and 84° in Zn were grown. Since tilt GBs with different ϕ possess different energy σ_{GB} , we also expected different T_w values for them. The bicrystals were cut into pieces of 10-mm length. The layer of the (Al)+(Zn) alloy of nearly eutectic composition was applied on two opposite surfaces of each $2 \times 10 \times 10$ mm Al and Zn bicrystal. Individual $2 \times 10 \times 10$ mm Al and Zn bicrystals coated by a

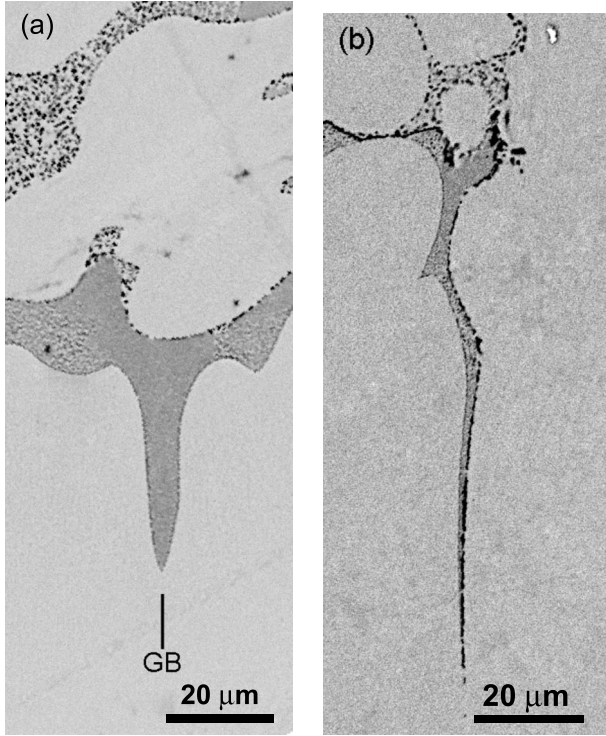
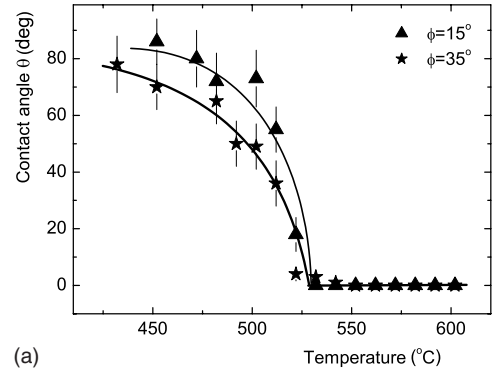


FIG. 3. Contact angle between $[11\bar{2}0]$ $\phi=46^\circ$ tilt GB in Zn (bottom part of the SEM micrographs, white) and Al-containing melt (upper part of the SEM micrographs, gray, quenched) at (a) 394°C and (b) 408°C .

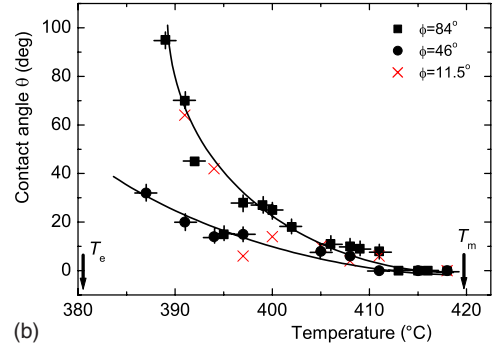
(Al)+(Zn) layer were sealed in the silica ampoules, evacuated to 10^{-4} Pa, and filled with high-purity argon. The coated Al bicrystals were annealed between 420 and 620°C for 1 h. The coated Zn bicrystals were annealed between 387 and 418°C for 1 h (for the liquid-phase wetting) and between 330 and 370°C for 720 h (for the solid-phase wetting). After annealing the samples were quenched in cold water, sectioned perpendicular to the GB and coated surfaces, embedded into metallographic resin and ground, and polished. The microstructure was investigated with the aid of scanning electron microscopy (SEM) and light microscopy (LM). SEM investigations were carried out in a Tescan Vega TS5130 MM microscope equipped with the LINK energy-dispersive spectrometer produced by Oxford Instruments. LM was performed using a Neophot-32 light microscope equipped with a 10 Mpix Canon Digital Rebel XT camera. In Fig. 3 the contact angle θ formed by the Al-containing melt at the $[11\bar{2}0]$ $\phi=46^\circ$ tilt GB in Zn after annealing at 394°C and 408°C is shown as an example.

III. EXPERIMENTAL RESULTS

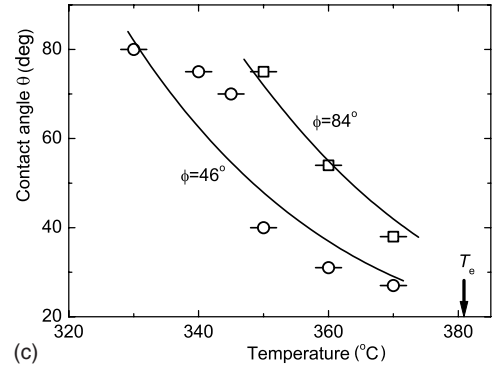
The contact angle θ decreases with increasing temperature in all three experimental series [Figs. 4(a)–4(c)]. In the case of Al GBs, the contact angle starts from about $\theta=80^\circ$, decreases with increasing temperature, and reaches $\theta=0^\circ$ at $T_{w15^\circ}=525^\circ\text{C}$ for $\phi=15^\circ$ and at $T_{w35^\circ}=530^\circ\text{C}$ for $\phi=35^\circ$ [Fig. 4(a)]. Above T_{w15° and T_{w35° , the contact angle remains zero. Both T_{w15° and T_{w35° lie between $T_{wsGB0\%}$ and



(a)



(b)



(c)

FIG. 4. (Color online) Temperature dependences of contact angle θ for (a) Al GBs in the contact with Zn-rich melt; (b) Zn GBs in the contact with Al-rich melt; and (c) Zn GBs in the contact with the $(\text{Al})''$ solid phase.

$T_{wsGB100\%}$ (Fig. 1). The $\theta(T)$ dependence for both Al GBs is convex. The first temperature derivative of each $\theta(T)$ dependence (and, respectively, of the GB energy) has a break at T_{w15° and T_{w35° . The convex shape and the break of the temperature derivative for $\theta(T)$ were predicted for the first-order (discontinuous) wetting transitions.⁵ In the case of the liquid-phase wetting of Zn GBs, the contact angle starts from about $\theta=80^\circ$, decreases with increasing temperature, and reaches $\theta=0^\circ$ at $T_{w46^\circ}=T_{w11.5^\circ}=415^\circ\text{C}$ for the $\phi=46^\circ$ and $\phi=11.5^\circ$ and at $T_{w84^\circ}=418^\circ\text{C}$ for $\phi=84^\circ$ [Fig. 4(b)]. Above T_{w46° , $T_{w11.5^\circ}$, and T_{w84° , the contact angle remains zero. The $\theta(T)$ dependence for all three Zn GBs is concave. The first temperature derivative of each $\theta(T)$ dependence (and, respectively, of the GB energy) remains continuous at T_{w46° , $T_{w11.5^\circ}$, and T_{w84° . The concave shape and the continuity of the temperature derivative for $\theta(T)$ were predicted for the second-order (continuous) wetting transitions.⁵

In the case of the solid-phase wetting of Zn GBs, the contact angle starts from about $\theta=80^\circ$, decreases with increasing temperature, and reaches $\theta=37^\circ$ for the GB with $\phi=46^\circ$ and $\theta=28^\circ$ for the GB with $\phi=84^\circ$ at $T=370^\circ\text{C}$. In other words, both studied GBs belong to the majority of GBs, which remain partially wetted by a second solid phase (Al)ⁿ below T_e .⁵⁶ However, the $\theta(T)$ dependence for both Zn GBs is concave. As mentioned above, the concave shape is an indication of the second-order (continuous) wetting transitions.⁵

IV. DISCUSSION

The convex shape and the break of the temperature derivative for $\theta(T)$ are usual for the GB wetting phase transformations.⁸⁻¹⁴ However, the concave shape and the continuous temperature derivative for $\theta(T)$ are observed for the GB wetting. Theory also predicts different critical exponents, namely, 1/2 for the discontinuous and 3/2 for the continuous wetting transitions.⁵ In Fig. 5 the measured $\theta(T)$ dependences (Fig. 4) are presented in the scaling coordinates $\log \theta - \log[(T - T_w)/T_w]$. Data for Al GBs fit well to the slope 1/2 [Fig. 5(a)]. A line with the slope 3/2 is also shown for comparison. In other words, the scaling condition for the discontinuous transition is fulfilled for the wetting of Al GBs by the Zn-rich melt. The scaling exponent of 1/2 for GB wetting transition was also observed for similar tilt Al GBs wetted by the Sn-rich melt.¹³ Temperature dependences $\theta(T)$ for two different tilt GBs were convex and the break of the temperature derivative for $\theta(T)$ was also present.¹³

Data for Zn GBs fit well to the slope 3/2 [Figs. 5(b) and 5(c)]. It concerns both GB wetting by a liquid phase (filled symbols) and by a second solid phase (open symbols). The extrapolated values $T_{ws46^\circ}=415^\circ\text{C}$ and $T_{ws84^\circ}=410^\circ\text{C}$ were used for the GB wetting in Zn by the (Al)ⁿ solid phase [Figs. 5(b) and 5(c)]. Lines with the slope 1/2 are also shown for comparison. In other words, the scaling condition for the continuous transition is fulfilled for the wetting of Zn GBs by the Al-rich melt and the (Al)ⁿ solid phase.

The experiments with Zn-5 wt % Al polycrystalline alloys showed that the first Zn/Zn GBs become completely wetted by the (Al)ⁿ solid phase at $T_{wsGB0\%}=290^\circ\text{C}$ (see also Fig. 1).⁵⁶ However, only about 30% of all Zn/Zn GBs become wetted at the eutectic temperature $T_e=381^\circ\text{C}$. These GBs possess the highest energy among all GBs in Zn polycrystal. The Zn/Zn GBs with low energy (such as twin GBs) remained incompletely wetted at T_e .⁵⁶ In the Al-rich alloys, all high-angle GBs become wetted above $T_{wGB100\%}=565^\circ\text{C}$ (Fig. 1).⁵³ The minimum temperature of GB wetting phase transition for Al/Al GBs is $T_{wGB0\%}=440^\circ\text{C}$ (Fig. 1).¹⁹ The temperatures of GB wetting for tilt GBs grown in this work, $T_{w35^\circ}=530^\circ\text{C}$ and $T_{w15^\circ}=525^\circ\text{C}$, are very close to the maximum temperature $T_{wGB100\%}$ and are far away from the minimum one $T_{wGB0\%}$ (Fig. 1). On the other hand, it is known that the energy difference between GBs with the misorientation angles of 15° and 35° is maximal possible for the $\langle 110 \rangle$ tilt GBs.⁶¹ It means that all tilt GBs possess rather low energies, comparable with general GBs in a polycrystal. Therefore, it is not surprising that all three $[11\bar{2}0]$ tilt Zn

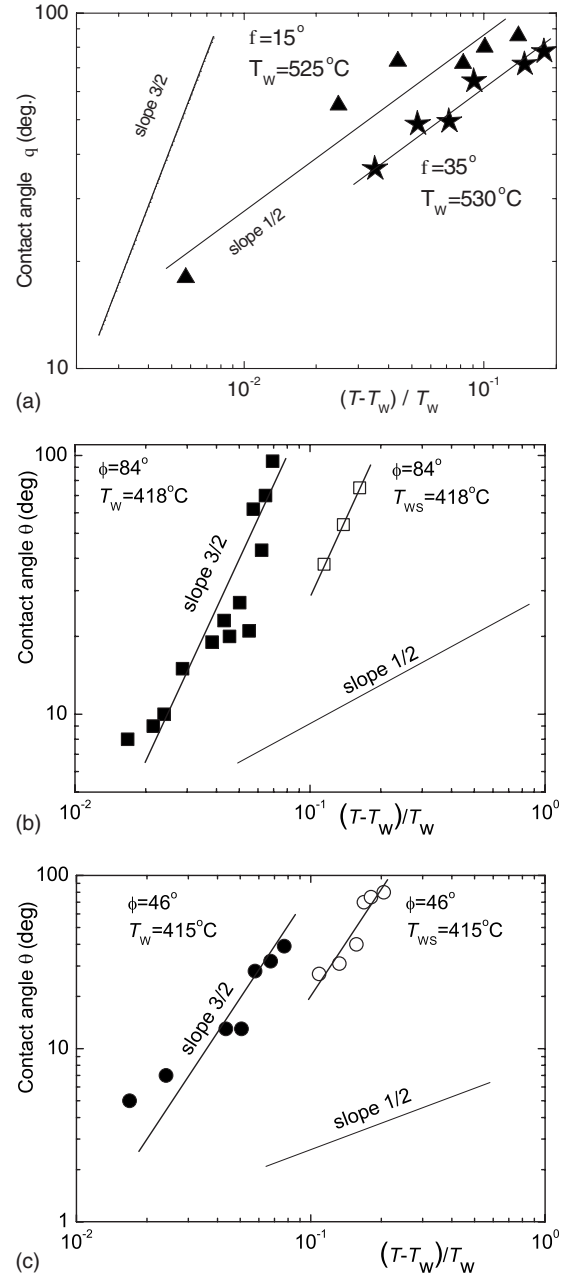


FIG. 5. Temperature dependences of the contact angle θ (same symbols as in Fig. 4) in scaling coordinates.

GBs grown in this work belong to the 70% of GBs, which remain partially wetted at T_e . It is especially true since the $84^\circ [11\bar{2}0]$ tilt GB is very close to the twin GB having minimum possible energy among all GBs in Zn. Therefore, the T_{ws} value for such GBs was estimated using the extrapolation to the temperatures above T_e [Figs. 4(c), 5(b), and 5(c)]

If the concave shape and the continuous temperature derivative for $\theta(T)$ [Figs. 4(b) and 4(c)] undoubtedly witness that the GB wetting transition in Zn-rich samples is continuous, then the scaling exponent of 3/2 [Figs. 5(b) and 5(c)] deserves more detailed discussion. Namely, the 3/2 exponent is predicted for critical wetting in systems whose wetting behavior is governed by long-range forces (more specifically nonretarded dispersion force) (see Sec. IVB of Ref. 5). How-

ever, wetting in metallic systems is usually thought to be controlled by short-range forces rather than by dispersion force and wetting theory does not predict a universal scaling exponent $3/2$ for such systems (see Sec. IIIB-D of Ref. 5). Therefore, the observed $3/2$ exponent could be either a coincidence or indeed an indication that long-range force controls the wetting behavior of Zn GB by Al melt. Surely, the second possibility would be more interesting. It can be experimentally checked, namely, since the dispersion force is also weak in metals, one can expect that Zn GBs will be quite thick (a few tens of atomic layers) just below the wetting point—similar to the mesoscale alkane films on water systems.³⁸ The presence of “thick” GBs or GB prewetting films was already witnessed by both direct or indirect experiments in the metallic systems such as the Al-rich Al-Zn alloys,^{54,55,58} Cu-Bi,^{18,62} or Fe-Si-Zn alloys.^{15–17} The direct observation of the thick GBs in the Zn-rich Zn-Al alloys just below the wetting point would convincingly prove the importance of long-range force to GB wetting in metals. Such experiments using the synchrotron radiation will be performed by us soon. They have to be conducted *in situ* by the very exact temperature control.

Thus, we observed that in the Al-Zn system, the change from the discontinuous GB wetting in the Al-rich side to the continuous GB wetting in the Zn-rich side proceeds. In Ref. 63 the multilayer adsorption on attractive substrates was analyzed. Various combinations of substrate-liquid interaction energy and interaction between atoms in the liquid phase have been compared. It has been theoretically predicted that in the case of strong substrate-liquid interaction and weak liquid-liquid interaction, the wetting should be of the first order. However, if substrate-liquid interaction becomes weaker, then the wetting transition can become continuous.⁶³ The interatomic force in a metal correlates well with a melting temperature. Similar to the ideas in Ref. 63, Al ($T_{mAl} = 660.45$ °C) can be considered as a stronger substrate and Zn ($T_{mZn} = 419.58$ °C) would represent a weaker one. The transition from Al GBs to Zn GBs leads to the change from discontinuous to continuous wetting. Again, similar to the case of critical exponent $3/2$, Ref. 63 only considered the long-range interaction between substrate and adsorbate. On

the first glance, it does not suit well metallic systems. Therefore, the future experimental search for possible thick GBs just below the wetting point in Zn-rich Zn-Al alloys will give the crucial proof for the presence of long-range interaction in metallic GBs.

Previously only the wetting of GBs in metals with high T_m by a melt based on a low- T_m metal has been studied (i.e., in a “large ear” of a eutectic phase diagram).^{8–14} Therefore, the convex $\theta(T)$ and discontinuities of $d\theta/dT$ at T_w were always observed (first-order transitions). Already an attempt to study the wetting of GBs in a low- T_m metal by a liquid phase containing atoms of a high- T_m metal enabled us to find the continuous GB wetting. Most probably, the continuous GB wetting transitions are hidden in the “small ears” of other eutectic phase diagrams.

V. CONCLUSIONS

By measuring the temperature dependences of the contact angle $\theta(T)$ between (i) specially grown tilt grain boundaries in Al and the Zn-rich melt; (ii) tilt GBs in Zn and the Al-rich melt; and (iii) tilt GBs in Zn and the Al-based solid solution (Al)ⁿ, the discontinuous and continuous GB wetting transitions were observed. The wetting transformation for Al GBs is discontinuous (first order): $\theta(T)$ dependence is convex, $d\theta/dT$ has a break at T_w , and $\theta \sim [(T - T_w)/T_w]^{1/2}$. The wetting transformation for Zn GBs is continuous: $\theta(T)$ dependence is concave, $d\theta/dT$ is continuous at T_w , and $\theta \sim [(T - T_w)/T_w]^{3/2}$. For the Zn GBs in contact with a second solid phase (Al)ⁿ, $\theta(T)$ dependence is concave and $\theta \sim [(T - T_w)/T_w]^{3/2}$ for the extrapolated T_w . The critical exponent of $3/2$ may indicate that GB wetting in the Zn-rich alloys is governed by the long-range forces.

ACKNOWLEDGMENTS

The authors thank Prof. S. Dietrich for the inspiring discussions and Mrs. J. Breithaupt for the language improvement. The Russian Foundation for Basic Research (Contracts No. 05-02-16528 and No. 08-08-90105), the INTAS (Contracts No. 05-1000008-8120 and No. 05-109-4951), and the German Federal Ministry for Education and Research are acknowledged for their financial support.

¹J. W. Cahn, J. Chem. Phys. **66**, 3667 (1977).

²C. Ebner and W. F. Saam, Phys. Rev. Lett. **38**, 1486 (1977).

³P. G. de Gennes, Rev. Mod. Phys. **57**, 827 (1985).

⁴D. E. Sullivan and M. M. Telo da Gama, in *Fluid Interfacial Phenomena* edited by C. A. Croxton (Wiley, New York, 1986).

⁵S. Dietrich, in *Phase Transitions and Critical Phenomena*, edited by C. Domb and J. L. Lebowitz (Academic, London, 1988), Vol. 12.

⁶M. Schick, in *Liquids at Interfaces (Les Houches Session XLVIII, 1988)* edited by J. Charvolin, J.-F. Joanny, and J. Zinn-Justin (Elsevier, Amsterdam, 1990).

⁷D. Bonn and D. Ross, Rep. Prog. Phys. **64**, 1085 (2001).

⁸A. Passerone, N. Eustathopoulos, and P. Desré, J. Less-Common

Met. **52**, 37 (1977).

⁹A. Passerone, R. Sangiorgi, and N. Eustathopoulos, Scr. Metall. **16**, 547 (1982).

¹⁰N. Eustathopoulos, Int. Met. Rev. **28**, 189 (1983).

¹¹B. B. Straumal, *Grain Boundary Phase Transitions* (Nauka, Moscow, 2003) (in Russian).

¹²B. Straumal, T. Muschik, W. Gust, and B. Predel, Acta Metall. Mater. **40**, 939 (1992).

¹³B. Straumal, D. Molodov, and W. Gust, Interface Sci. **3**, 127 (1995).

¹⁴B. Straumal, W. Gust, and T. Watanabe, Mater. Sci. Forum **294-296**, 411 (1999).

¹⁵E. I. Rabkin, V. N. Semenov, L. S. Shvindlerman, and B. B.

- Straumal, *Acta Metall. Mater.* **39**, 627 (1991).
- ¹⁶O. I. Noskovich, E. I. Rabkin, V. N. Semenov, B. B. Straumal, and L. S. Shvindlerman, *Acta Metall. Mater.* **39**, 3091 (1991).
- ¹⁷B. B. Straumal, O. I. Noskovich, V. N. Semenov, L. S. Shvindlerman, W. Gust, and B. Predel, *Acta Metall. Mater.* **40**, 795 (1992).
- ¹⁸L.-S. Chang, E. Rabkin, B. B. Straumal, B. Baretzky, and W. Gust, *Acta Mater.* **47**, 4041 (1999).
- ¹⁹B. Straumal, G. López, W. Gust, and E. Mittemeijer, in *Nanomaterials by Severe Plastic Deformation. Fundamentals—Processing—Applications*, edited by M. J. Zehetbauer and R. Z. Valiev (VCH, Weinheim/Wiley, New York, 2004).
- ²⁰G. Pezzotti, A. Nakahira, and M. Tajika, *J. Eur. Ceram. Soc.* **20**, 1319 (2000).
- ²¹Y. Furukawa, O. Sakurai, K. Shinozaki, and N. Mizutani, *J. Ceram. Soc. Jpn.* **104**, 900 (1996).
- ²²M. Elfving, R. Osterlund, and E. Olsson, *J. Am. Ceram. Soc.* **83**, 2311 (2000).
- ²³H. Wang and Y.-M. Chiang, *J. Am. Ceram. Soc.* **81**, 89 (1998).
- ²⁴I. Tanaka, H. J. Kleebe, M. K. Cinibuluk, J. Bruley, D. R. Clarke, and M. Ruhle, *J. Am. Ceram. Soc.* **77**, 911 (1994).
- ²⁵D. A. Molodov, U. Czubayko, G. Gottstein, L. S. Shvindlerman, B. B. Straumal, and W. Gust, *Philos. Mag. Lett.* **72**, 361 (1995).
- ²⁶B. Straumal, N. E. Sluchanko, and W. Gust, *Defect Diffus. Forum* **188-190**, 185 (2001).
- ²⁷S. H. Islam, X. Qu, and X. He, *Powder Metall.* **50**, 11 (2007).
- ²⁸D. Q. Wei, Q. C. Meng, and D. C. Jia, *Ceram. Int.* **33**, 221 (2007).
- ²⁹K. P. Solek, R. M. Kuziak, and M. Karbowniczek, *Arch. Metall. Mater.* **52**, 25 (2007).
- ³⁰Z. S. Ji, M. L. Hu, and X. P. Zheng, *J. Mar. Sci. Technol.* **23**, 247 (2007).
- ³¹Y. A. Shatilla and E. P. Loewen, *Nucl. Technol.* **151**, 239 (2005).
- ³²S. Dietrich and M. Schick, *Phys. Rev. B* **31**, 4718 (1985).
- ³³W. F. Saam and V. B. Shenoy, *J. Low Temp. Phys.* **101**, 225 (1995).
- ³⁴V. B. Shenoy and W. F. Saam, *Phys. Rev. Lett.* **75**, 4086 (1995).
- ³⁵S. Dietrich and M. Napiorkowski, *Phys. Rev. A* **43**, 1861 (1991).
- ³⁶J. O. Indekeu and J. M. J. van Leeuwen, *Physica C* **251**, 290 (1995); *Physica A* **236**, 114 (1997).
- ³⁷C. J. Boulter and F. Clarysse, *Phys. Rev. E* **60**, R2472 (1999).
- ³⁸K. Ragil, J. Meunier, D. Broseta, J. O. Indekeu, and D. Bonn, *Phys. Rev. Lett.* **77**, 1532 (1996).
- ³⁹N. Shahidzadeh, D. Bonn, K. Ragil, D. Broseta, and J. Meunier, *Phys. Rev. Lett.* **80**, 3992 (1998).
- ⁴⁰D. Ross, D. Bonn, and J. Meunier, *Nature (London)* **400**, 737 (1999).
- ⁴¹T. Pfohl and H. Riegler, *Phys. Rev. Lett.* **82**, 783 (1999).
- ⁴²E. Bertrand, H. Dobbs, D. Broseta, J. O. Indekeu, D. Bonn, and J. Meunier, *Phys. Rev. Lett.* **85**, 1282 (2000).
- ⁴³D. Ross, D. Bonn, and J. Meunier, *J. Chem. Phys.* **114**, 2784 (2001).
- ⁴⁴S. Rafai, D. Bonn, E. Bertrand, J. Meunier, V. C. Weiss, and J. O. Indekeu, *Phys. Rev. Lett.* **92**, 245701 (2004).
- ⁴⁵S. Rafai, D. Bonn, and J. Meunier, *Physica A* **358**, 97 (2005).
- ⁴⁶P. S. Swain and A. O. Parry, *Europhys. Lett.* **37**, 207 (1997).
- ⁴⁷A. O. Parry and P. S. Swain, *Physica A* **250**, 167 (1998).
- ⁴⁸J. O. Indekeu, K. Ragil, D. Bonn, D. Broseta, and J. Meunier, *J. Stat. Phys.* **95**, 1009 (1999).
- ⁴⁹F. Clarysse and C. J. Boulter, *Physica A* **278**, 356 (2000).
- ⁵⁰A. Sartori and A. O. Parry, *J. Phys.: Condens. Matter* **14**, L679 (2002).
- ⁵¹W. Fenzl, *Europhys. Lett.* **64**, 64 (2003).
- ⁵²A. Yochelis and L. M. Pismen, *Colloids Surf., A* **274**, 170 (2006).
- ⁵³B. B. Straumal, O. Kogtenkova, and P. Zięba, *Acta Mater.* **56**, 925 (2008).
- ⁵⁴B. B. Straumal, A. A. Mazilkin, O. A. Kogtenkova, S. G. Protasova, and B. Baretzky, *Philos. Mag. Lett.* **87**, 423 (2007).
- ⁵⁵B. Straumal, O. Kogtenkova, S. Protasova, A. Mazilkin, P. Zieba, T. Czeppe, J. Wojewoda-Budka, and M. Faryna, *Mater. Sci. Eng., A* (to be published 2008).
- ⁵⁶G. A. López, E. J. Mittemeijer, and B. B. Straumal, *Acta Mater.* **52**, 4537 (2004).
- ⁵⁷*Binary Alloy Phase Diagrams*, edited by T. B. Massalski, J. L. Murray, L. H. Bennett, and H. Baker (ASM International, Materials Park, OH, 1993).
- ⁵⁸B. Straumal, R. Valiev, O. Kogtenkova, P. Zieba, T. Czeppe, E. Bielanska, and M. Faryna, *Acta Mater.* (to be published 2008).
- ⁵⁹O. A. Kogtenkova, B. B. Straumal, S. G. Protasova, and P. Zięba, *Defect Diffus. Forum* **237-240**, 603 (2005).
- ⁶⁰B. B. Straumal, V. G. Sursaeva, and A. S. Gornakova, *Z. Metallkd.* **96**, 1147 (2005).
- ⁶¹G. C. Hasson and C. Goux, *Scr. Metall.* **5**, 889 (1971).
- ⁶²S. V. Divinski, M. Lohmann, Chr. Herzig, B. Straumal, B. Baretzky, and W. Gust, *Phys. Rev. B* **71**, 104104 (2005).
- ⁶³R. Pandit, M. Schick, and M. Wortis, *Phys. Rev. B* **26**, 5112 (1982).